

Cite this: *Soft Matter*, 2011, **7**, 10694[www.rsc.org/softmatter](http://www.rsc.org/softmatter)

PAPER

# Pickering emulsions stabilized by stacked catanionic micro-crystals controlled by charge regulation†

Natascha Schelero,<sup>a</sup> Antonio Stocco,<sup>b</sup> Helmuth Möhwald<sup>b</sup> and Thomas Zemb<sup>c</sup>

Received 18th April 2011, Accepted 8th August 2011

DOI: 10.1039/c1sm05689a

In this paper the mechanism behind the stabilization of Pickering emulsions by stacked catanionic micro-crystals is described. A temperature-quench of mixtures of oppositely charged surfactants (catanionics) and tetradecane from above the chain melting temperature to room temperature produces stable oil-in-water (o/w) Pickering emulsions in the absence of Ostwald ripening. The oil droplets are decorated by stacks of crystalline discs. The stacking of these discs is controlled by charge regulation as derived from conductivity, scattering and zeta potential measurements. Catanionic nanodiscs are ideal solid particles to stabilize Pickering emulsions since they present no density difference and a structural surface charge which is controlled by the molar ratio between anionic and cationic components. The contact angle of catanionic nanodiscs at a water/oil interface is also controlled by the non-stoichiometry of the components. The resulting energy of adhesion and the repulsion between droplets is much larger than kT. As a consequence of these unique properties of nanodiscs, this type of emulsions presents an extremely high resistance towards coalescence and creaming, even in the presence of salt.

## 1. Introduction

Emulsions stabilized by particles are called solid-stabilized emulsions or Pickering-emulsions, because in 1907, Pickering generalized the initial observations by Perrin and Ramsden that fine solid particles wetted by water rather than oil act as emulsifiers for o/w emulsions by residing at the interface.<sup>1</sup> Since then, properties of micro and nano particles which are ideally suited for stabilizing Pickering emulsions have been identified. The adsorption of particles at the oil/water interface strongly depends on the particle size and shape, wettability, and interparticle interaction.<sup>2,3</sup> Furthermore, such particles must have (1) negligible solubility in water and in oil, even with a high specific surface, so that a transition from particle to molecules *via* leaching or chemical dissolution does not occur, (2) a density at best in between water and oil to avoid density gradients, and (3) known contact angles with water and oil close to 90° in order to induce surface tension reduction between the two phases of the emulsion.

Interestingly, the known properties of catanionic crystals produced in the salt-free system made from weak carboxylic

acids and alkyltrimethylammonium hydroxides, uniquely fulfil these four requirements:

1. the density gradient is negligible, since their components have densities between water and many oils;
2. the osmotic repulsion between discs is known;<sup>4</sup>
3. the local crystalline in plane order is known;<sup>5</sup>
4. the ternary phase prism important for the determination of the temperature range for preparing and storing the emulsions is known.<sup>6,7</sup>

For these reasons, catanionics seem to be a powerful emulsifier. In general, the term catanionics describes on the one hand, systems where cationic and anionic surfactants are mixed in non-equimolar ratios with their counterions present.<sup>8</sup> In these mixtures, the catanionic surfactant coexists as an individual chemical species with an equimolar amount of salt and excess of one of the ionic components. On the other hand, catanionics are formed from pairing two oppositely charged surfactants with removal of the inorganic counterions by ion-exchange, precipitation or extraction at equimolar quantities.<sup>9</sup> Even though it was empirically known since the early seventies that mixtures of oppositely charged surfactants and lipid formulations are extremely efficient emulsifiers, emulsions stabilized by catanionics have been rarely mentioned in the literature.<sup>10–16</sup> This is even more astonishing since it is proposed that catanionics might combine the advantages of particle stabilization of emulsions and the amphiphilicity of molecular surfactants to afford better emulsion stabilization. This unique property is else only known for the so-called “Janus” particles.<sup>17</sup> Previously, the authors ascertained the proposed extraordinary high lifetime of Pickering

<sup>a</sup>Stranski-Laboratorium, Department of Chemistry, TU Berlin, Strasse des 17. Juni 124, 10623 Berlin, Germany

<sup>b</sup>Max-Planck-Institut für Kolloid- und Grenzflächenforschung, Am Mühlenberg 1, 14424 Potsdam, Germany

<sup>c</sup>Institut de Chimie Séparative de Marcoule UMR 5257, CEA/CNRS/UM2/ENSCM, Marcoule, France

† Electronic supplementary information (ESI) available. See DOI: 10.1039/c1sm05689a

emulsions stabilized by catanionic crystals due to particle-by-particle counting *via* light scattering.<sup>16</sup> The aim of this paper is to gain a general understanding of the mechanism governing the stability of emulsions stabilized by catanionic crystals.

Furthermore, the resilience of such emulsions against external influences like salt is tested.

## 2. Experimental methods

### 2.1 Materials

We chose tetradecane as oil because its low solubility renders negligible the ripening mechanism by molecular exchange.<sup>18</sup> Tetradecane (Fluka, p.a. > 99%) was used as received. Water was passed through a reverse osmosis unit and a Milli-Q reagent water system. A 10 wt% solution of hexadecyltrimethylammonium hydroxide (CTAOH) in water (Fluka) was freeze-dried, recovered in a minimum amount of ethanol and recrystallized twice from anhydrous ether in order to remove the impurities due to self-decomposition of CTAOH, mainly trimethylamine and hexadecane resulting from Hoffmann elimination. Myristic acid (Fluka, p.a. >99%) was recrystallized twice from hot acetonitrile.

### 2.2 Sample preparation

**2.2.1 Catanionic solutions.** The catanionic solutions were prepared following the standard procedure as reported in several publications.<sup>4,6,7,19–22</sup> In general, catanionic systems are specified by three characteristic quantities: (1) the total amount of dry surfactant  $c$  in wt%, (2) the molar ratio of anionic surfactant  $r$ , and (3) the fraction of counterions exchanged from original  $\text{OH}^-$  to  $\text{Cl}^-$   $x$ . In order to adjust the desired amount of ions – in the presented cases  $x = 5.3\%$ , CTAOH and CTACl were mixed as powders in the required ratio, solved in small amounts of water and then lyophilized. To prepare the catanionic solutions, the desired amount of CTAOH/CTACl is weighed, then myristic acid is added to receive the desired  $r$ -value and finally the missing amount of water is filled up in order to gain the wanted concentration  $c$  of surfactant. After that the samples have to be heated above 50 °C to dissolve myristic acid. Short heating to 65 °C allows homogenisation of the sample and rearrangement of the surfactant chains.

**2.2.2 Emulsions.** Depending on the oil/water ratio the needed volume was put in a tube. The samples containing oil, water and catanionics were mixed for 2 min with a vortex-apparatus and then emulsified for 7 min by using an Ultra-Turrax T8 (Ika) while heating the sample in a water bath. The used dispersing machine works with a rotor–stator configuration, with a 5 mm head operating at a shearing speed of 49 700  $\text{s}^{-1}$ . During dispersion the samples were heated above the chain melting temperature since the used catanionic formulations are in the crystallized state ( $L_c$ ) at room temperature. As already known from earlier work, the chain melting temperature depends on the molar ratio of the anionic surfactant.<sup>7</sup> Thus, the samples with  $r < 0.5$  were heated up to 35–40 °C and the samples with  $r \geq 0.5$  above 65 °C. After dispersion the samples were cooled to room temperature and stored at a constant temperature of 20 °C. To perform measurements the emulsions had to be diluted with water by

different factors depending on the method used. Observation of various oil droplets showed that the characteristics of such droplets has never changed by diluting with water by different dilution factors.

### 2.3 Methods

**2.3.1 Confocal laser scanning microscopy (CLSM).** The emulsion droplets were visualized by an inverted confocal microscope IX 61 from Olympus with a FV 1000 confocal head equipped with a 100× oil immersion objective. In the present experiments we employed a combination of fluorescence and confocal microscopy. Therefore a fluorescent marker was added to all examined samples. The fluorescence of Oregon Green was excited by a 488 nm laser line. To reduce the high optical density for any confocal microscopic observation, the emulsions were diluted either 1 : 100 or 1 : 1000 by water. Five drops of Oregon green solution per 1 ml diluted emulsion were added. The concentration of the dye depends on the dilution factor of the emulsion. One drop of the prepared dilution containing the dye was put on a glass slide and covered with a second glass slide. The glass slides were stuck together to avoid too fast evaporation of the small sample under the microscope.

**2.3.2 Electrophoretic mobility.** The electrophoretic mobility was achieved by using a Zetasizer Nano Z (Malvern Instruments). For measuring, the emulsions were diluted by water by a factor 1 : 1000 and measured in a Folded Capillary cell DTS 1060—a maintenance-free capillary cell. For comparison, several experiments were repeated with a Zetasizer 3000 HS (Malvern Instruments). The Smoluchowski formula

$$U_E = \frac{\zeta \varepsilon \varepsilon_0}{\eta} \quad (1)$$

where  $\eta$  is the the viscosity of the solvent,  $\varepsilon_0$  is the dielectric permittivity in vacuum, and  $\varepsilon$  is the relative dielectric permittivity of the solvent, was used to relate the electrophoretic mobility,  $U_E$ , with the droplet's  $\zeta$ -potential.

**2.3.3 Conductivity measurements.** The conductivity of the emulsions and the catanionic solutions was in all cases determined using a CDM 210 digital conductivity meter with Pt/Pt electrodes for micro samples. The emulsions were kept in tubes for at least 20 days which were turned upside down and the different phases were extracted carefully, filled in Eppendorf cups and measured with this electrode for microsamples.

**2.3.4 Interfacial tension and contact angle experiments.** Interfacial tension was measured by the capillary pressure technique (DPA, Sinterface, Germany). In this method, the interfacial tension is calculated from the pressure measured by a pressure sensor. Additionally, the shape and the volume of the droplet formed at the tip of a capillary can be monitored in time by means of a camera.<sup>23</sup> First, we measured the interfacial tension of the bare water–tetradecane interface ( $\gamma_{\text{TW}} = 52.9 \text{ mN m}^{-1}$ ) to check the purity of the liquids used. Then, we measured the interfacial tensions of concentrated aqueous catanionic solutions against tetradecane.

The contact angles of tetradecane droplets on catanionic substrates were measured by a commercial apparatus (G10, Krüss, Germany).

### 3. Results

As mentioned above, the obtained emulsions remain re-dispersible irrespective of the ratio of the catanionic solution and the formulation. The reason for this particular behavior is that the anionic and cationic surfactants used as catanionics interact with typically 10 kT per amphiphilic pair, resulting in a monomer concentration range from 1 to 10  $\mu\text{M}$ . Due to these ultra-low “cmc” (critical micelle concentration) or “cac” (critical aggregate concentration) values for salt-free catanionics,<sup>24</sup> the investigated emulsions can be diluted since only very little amounts of the micro crystals present are solubilized.

Fig. 1 depicts the observation of diluted samples by CLSM microscopy which is straightforward in case of droplets in the range of 1 to 5  $\mu\text{m}$ .

The catanionic mixture used contains a tiny amount of a fluorescent lipid-based dye (Oregon green). The mono-dispersity of the size can be estimated from the low magnification picture, while at higher magnification, it appears that each fluorescent patch has typically five neighbors, meaning that twelve patches typically cover an oil droplet. This can be either in order to minimize the bending energy or because of a topological reason. On a molecular scale, a six fold symmetry in the surface plane must be broken at least twelve times to form a closed sphere. The typical solid angle covered by each apparent particle from the center is therefore around  $4\pi/12$ .

From the phase diagram and WAXS/WANS (wide angle X-ray/neutron) experiments it is known that these aggregates are crystalline. All emulsions are prepared at temperatures above the melting temperature as shown in the complete phase prism.<sup>7</sup>

Moreover, semi-flexible discs are the ideal shape for stabilizing Pickering emulsions since they can accommodate any contact angle due to the high curvature of their hydrophilic edges. According to the literature, the thickness of one catanionic bilayer is 4 nm while SANS experiments using contrast variation have shown that less than ten discs are stacked in one “particle” stabilizing the emulsions.<sup>16</sup> In order to relate both measurements more quantitative information about the amount of material present at the liquid/liquid interface is needed.

Direct application of the Gibbs equation is not possible due to the low solubility. However, surface tension measurements at the air/water interface showed a strong increase in surface pressure  $\Pi = \gamma_{\text{AW}} - \gamma = 45\text{--}46 \text{ mN m}^{-1}$  ( $\gamma_{\text{AW}} = 72 \text{ mN m}^{-1}$ ).<sup>25</sup> Here, the water/oil interfacial tension as a function of time is deduced from the capillary pressure of a water droplet in oil for two different compositions (Fig. 2). The capillary pressures which have been established slowly, are reduced by a factor of ten in the presence of catanionic micro crystals. As can be seen in Fig. 4, the zeta-potential of catanionic nanodiscs decreases from around +47 mV for  $r = 0.4$  with increasing molar ratio of anionic surfactant,  $r$ , to  $-25 \text{ mV}$  for  $r = 0.7$ . Thus, catanionic nanodiscs containing an excess of the cationic component should be more attracted to the tetradecane/water interface since the water/oil interface is negatively charged.<sup>26,27</sup> However, the results of the interfacial tension measurements (Fig. 2) indicate the opposite. It is assumed that a part of the myristic acid which is not needed after the rearrangement of the nanodiscs at the water/oil interface, dissolves in tetradecane since myristic acid easily dissolves in the oil phase but hardly in the water phase. This can lower the interfacial tension beside the adsorption of the catanionic nano discs. Therefore, the interfacial tension of  $r = 0.6$  appears lower than that of  $r = 0.4$ . In the present case, the surface pressure  $\Pi = \gamma_{\text{TW}} - \gamma = 49\text{--}53 \text{ mN m}^{-1}$  (see  $\gamma$  in Fig. 2) is very high and approaches the value of the bare interfacial tension ( $\gamma_{\text{TW}} = 52.9 \text{ mN m}^{-1}$ ).<sup>28</sup>

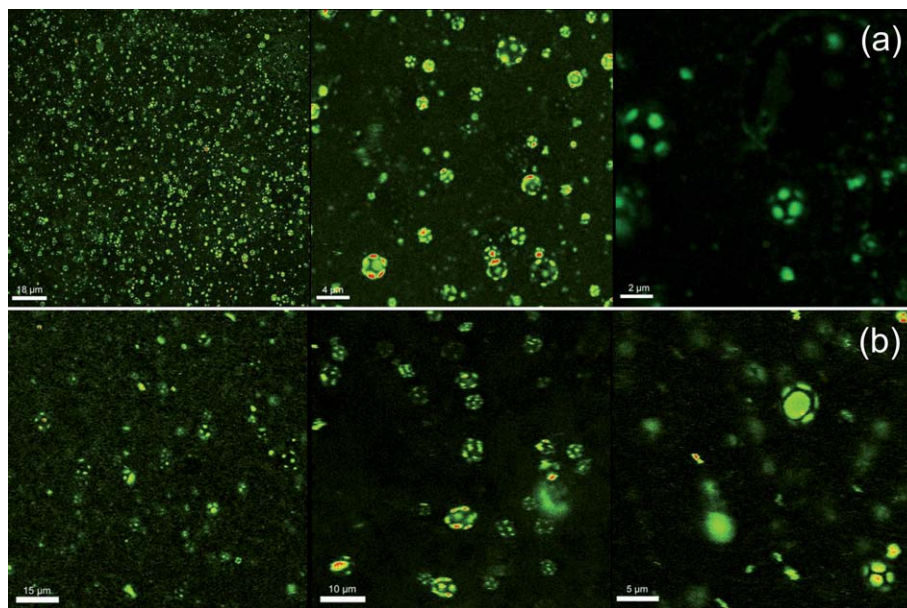


**Fig. 1** Tetradecane emulsion droplets stabilized by stacks of nanodiscs as seen by confocal microscopy with three different magnifications. Discs are labeled with Oregon green, a lipid based fluorescent dye which mixes with the catanionic bilayer. Emulsions decorated with catanionic crystals with  $r = 0.4$  (a) and  $r = 0.6$  (b).

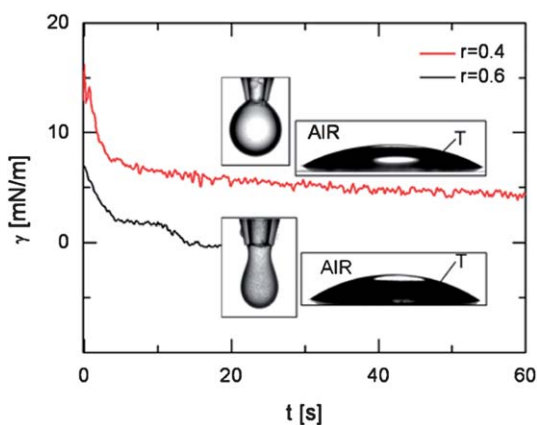


**Fig. 2** Interfacial tensions as a function of drop aging for  $r = 0.4$  and  $0.6$ . Central insets show an aqueous droplet in tetradecane during the capillary pressure experiment. Right insets show the contact angles of tetradecane (T) droplets on catanionic substrates. Top insets refer to  $r = 0.4$  and the lower to  $r = 0.6$ .

Whatever the molecular origin is, extreme reduction of water/tetradecane interfacial tension leads to long term emulsions stability, since the driving force towards coarsening is reduced.

Another way to obtain an average thickness of the discs is to follow the conductivity of the emulsions. In salt-free catanionics, conductivity is governed by “free” counter-ions since the surfactants in their monomer form as well, as the micro crystals as such do not contribute appreciably to the conductivity. As is usual with surfactant aggregates, ions partition between a physisorbed layer and “free” counter-ions in the double layer. In the absence of “Hofmeister” effect increasing the amount of bound cosmotropic ions, the free ions around micelles are typically  $2/3$  of the total ions present.<sup>29</sup>

The ratio of expected conductivity from a known amount of free counter-ions of the pure catanionic solutions *versus* measured conductivity of the emulsion indicates the amount of counter-ions adsorbed between stacked discs due to electro-neutrality, and hence the average number of discs. The raw data of the conductivity of emulsions and the corresponding catanionic solution without tetradecane droplets are given as ESI.† It is crucial to note that when two nanodiscs stack in a three-dimensional crystal, all counter-ions of the two stacked discs must be adsorbed. Thus stacking occurs best with the two compositions where local order is close to the one of anti-ferromagnetic materials with hexagonal symmetry (*i.e.*  $1/3$  and  $2/3$ ). As can be seen in Fig. 3, the relative conductivity significantly increases between  $r = 0.4$  and  $r = 0.6$ . The observed increase in relative conductivity corresponds to 60% ( $r = 0.4$ ) and 90% ( $r = 0.6$ ) of trapped ions in the catanionic aggregates around the oil droplet. Consequently, for  $r = 0.6$  typically ten discs are stacked which then form the nanoparticle firmly adsorbed at the surface of the oil droplets.

The corresponding thickness of the particle stabilizing the Pickering droplets is 40 nm, while the lateral expansion is of the order of 1  $\mu\text{m}$ . The ratio between the three axis of the solid particles is therefore 1-25-25. Any contact angle between 45 and 135° in the three tension line can be accommodated without attraction between particles or increase in water/oil contact area.

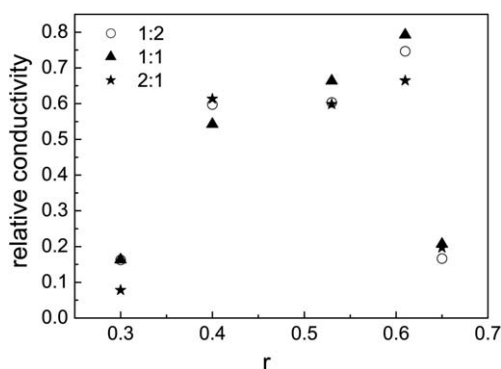


**Fig. 3** Relative conductivities of emulsions as a function of the ratio of anionic surfactant in the catanionic solutions ( $c = 1$  wt%) for three different values of oil/catanionic solution ratio. The relative conductivities were calculated by the conductivity of the emulsion over the conductivity of the corresponding catanionic solution.

Moreover, the stacking of discs does not change the zeta potential. As shown in Fig. 4, the zeta potentials measured as a function of molar ratio  $r$  demonstrates that the zeta potential is controlled by the composition of individual catanionic crystals. With increasing molar ratio of anionic component  $r$ , the zeta-potential decreases from +47 mV to  $-25$  mV. In the present case, the anionic component was myristic acid, a weak acid. Myristic acid has a  $\text{p}K_a \sim 5$  and tends to form dimers. Therefore, one can assume that in the catanionic samples considered, the myristic acid was not fully dissociated. For this reason, the amount of negative charges caused by the addition of anionic component can by no means be proportional to the amount of myristic acid added and charge reversal of the zeta potential occurs at  $r \gg 0.5$ .

After an exhaustive characterization of the stabilizing catanionic particles and long term stability experiments,<sup>16</sup> we can now turn to elucidating the mechanism of governing the stability of emulsions stabilized by such catanionic crystals.

As a first step, the energy of adsorption, in kT per particle, is derived from interfacial tension data and contact angle measurements.

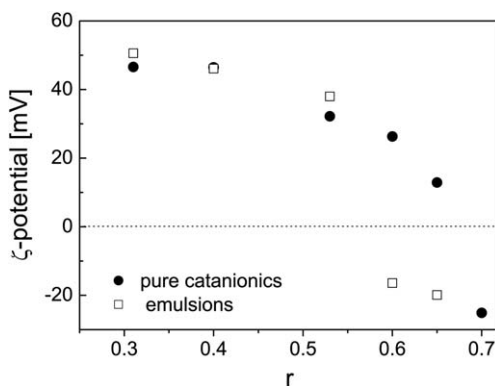


**Fig. 4** Zeta-potential  $\zeta$  as a function of the ratio of anionic surfactant  $r$  of diluted catanionic solutions (filled circles) and the corresponding emulsions (open squares). The catanionic solutions and emulsion were diluted by a factor 1 : 1000.

Equilibrium interfacial tensions  $\gamma_{0.4, \text{TW}} = 0 \pm 1 \text{ mN m}^{-1}$  and  $\gamma_{0.6, \text{TW}} = 4 \pm 1 \text{ mN m}^{-1}$  were measured for  $r = 0.4$  and  $r = 0.6$  by a capillary pressure technique at a relatively high cationic concentration  $c = 1 \text{ wt}\%$  (aqueous droplets in tetradecane are shown in Fig. 2). Moreover, the macroscopic contact angles of tetradecane drops on  $r = 0.4$  and  $r = 0.6$  substrates are  $\Theta_{0.4, \text{AT}} = 38.0^\circ \pm 0.3$  and  $\Theta_{0.6, \text{AT}} = 32.0^\circ \pm 0.1$ , respectively (see insets in Fig. 2). Hence, the relations between surface energies for cationic layers, air (A) and tetradecane (T), can be written as:

$$\sigma_{0.4, \text{A}} = \sigma_{0.4, \text{T}} + \gamma_{\text{AT}} \cos(\Theta_{0.4, \text{AT}}) \quad (2)$$

$$\sigma_{0.6, \text{A}} = \sigma_{0.6, \text{T}} + \gamma_{\text{AT}} \cos(\Theta_{0.6, \text{AT}}) \quad (3)$$

At the air/water interface, the surface tensions of cationic mixtures show plateau values in a relatively large range of concentrations pointing to a compact cationic layer at the surface.<sup>25</sup> Thus, we estimated the surface energies  $\sigma_i$  for cationics from the equilibrium surface tensions  $\gamma_i$ <sup>25</sup> by applying Connor's equation:<sup>30–32</sup>

$$\sigma_i = \gamma_i \frac{1 + \beta(1 - \Phi)}{1 - \alpha(1 - \Phi)} \quad (4)$$

where  $\Phi$  is the molar fraction and  $\alpha$  and  $\beta$  are two empirical constants close to 1.

$$\sigma_{0.4, \text{A}} = \gamma_{\text{AW}}(\Phi \rightarrow 1) = 25 \pm 1 \text{ mN m}^{-1} \quad (5)$$

$$\sigma_{0.6, \text{A}} = \gamma_{\text{AT}}(\Phi \rightarrow 1) = 26 \pm 1 \text{ mN m}^{-1} \quad (6)$$

From eqn (2)–(6), one obtains  $\sigma_{0.4, \text{T}} = 4 \pm 1 \text{ mN m}^{-1}$  and  $\sigma_{0.6, \text{T}} = 3.5 \pm 1 \text{ mN m}^{-1}$ . In order to estimate the energy of adsorption one just needs to calculate the surface tension between cationics and water. Following the procedure described by Binks and Clint,<sup>28</sup> one obtains  $\sigma_{0.4, \text{W}} = 26.8 \pm 1 \text{ mN m}^{-1}$  and  $\sigma_{0.6, \text{W}} = 27.9 \pm 1 \text{ mN m}^{-1}$  (see ESI).<sup>†</sup>

The energy of adsorption per particle as a function of the disc-particle location ( $z$ -direction) is plotted in Fig. 5. Wetting energies are calculated following Pieranski's model and by supposing that the particle has an oblate shape of  $1 \mu\text{m}$  in diameter and

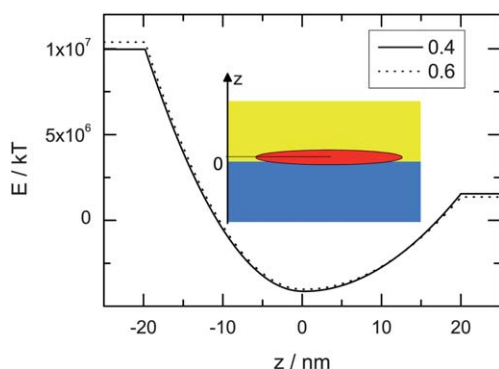


**Fig. 5** Energy of adsorption measured for an oblate particle ( $1 \mu\text{m}$  diameter and  $40 \text{ nm}$  thick) at the water/tetradecane interface.  $E(z) = \sigma_{\text{W}} A_{\text{W}}(z) + \sigma_{\text{T}} A_{\text{T}}(z) - \gamma_{\text{TW}} A_0(z)$ , where  $r = 0.4$  or  $0.6$ ;  $A_{\text{W}}(z)$ ,  $A_{\text{T}}(z)$  and  $A_0(z)$  are the areas of the oblate in water, tetradecane and the area removed to the bare interface, respectively. A contact angle close to  $90^\circ$  ( $z = 0$ ) and high adsorption energy  $E \gg kT$  are found for  $r = 0.4$  and  $r = 0.6$ .

a thickness of  $40 \text{ nm}$  so that the oblate exposes at maximum its surface to the interface.<sup>33</sup> Hence, a particle composed by a stack of nanodiscs adsorbs on an oil/water interface with an energy in the order of  $10^7 \text{ kT/particle}$ .

As a second step, the contact energy barrier can be estimated from the DLVO theory. The result is much larger than  $kT$ . Using the Schmoluchovki theory, the lifetime *versus* coalescence or creaming would be infinite. This means that in cationic stabilized emulsions, lifetime is limited by Ostwald ripening.

Finally, the resistance of the considered emulsion against external stimuli, in this case against salt, is tested. Therefore, the stability of two types of emulsions, namely,  $r = 0.4$  and  $r = 0.6$  with  $10^{-2} \text{ M NaCl}$ , has been followed for more than nine months. The practical stability of emulsions has been determined by monitoring droplet size distribution by SPLS<sup>16</sup> and concentration during storage as described by Weiss.<sup>34</sup>

Fig. 6 shows that in case of positively charged stacks of nanodiscs, the stability against coalescence and creaming after one month in the salt-free cationic system is limited to certain oil/cationic solution ratios. Namely, emulsions with a fraction of 25 to 55% of cationic solution remain completely stable. Indeed, those emulsions have been stable for more than 90 days.<sup>16</sup> Adding  $10^{-2} \text{ M}$  of  $\text{NaCl}$  induces a widening of the stability range. In this case, emulsions containing a fraction of 23% to almost 100% of cationic solution are remarkably stable. The authors are not aware of any other example of such extremely stable oil-rich emulsions in the absence of strongly adsorbed ionomers where the stability is enhanced by salt. The reason for the observed increase in stability due to salt addition is that stacking of nanodiscs is easier with salt. Moreover, the average thickness of stacks increases when salt is added. The energy barrier towards coalescence is still high, while the energy of adsorption is still  $\gg kT$ . The observed salt-resilience is a peculiarity of an emulsion stabilized by cationic crystals, since all other known cases of oil-in-water emulsions present a stability either insensitive or decreasing when salt is added. In contrast to this, cationic based Pickering emulsions stabilized by charged nanodiscs are much more stable in physiological conditions than in pure water.

By putting all presented results together, a clear picture of the stabilization mechanism associated with the structure of the cationic crystals emerges (see Fig. 7). The shape ratio 1-25-25 of the solid cationic crystals stabilizing the presented Pickering emulsions allows contact angle conditions which can be satisfied at a negligible cost of free energy.

## 4. Discussion

The mechanism of stacking between nanodiscs is easily found in a displacement of half a lattice vector in local hexagonal arrangements.<sup>5</sup> It is more surprising that stacks of discs do not facet appreciably the tetradecane droplets, although bending moduli are of the order of  $1 \text{ GPa}$ .<sup>35</sup> In principle, the stress  $\gamma/r$  induced by droplets of  $r = 1 \mu\text{m}$  and surface pressure  $\Pi = 4 \text{ mN m}^{-1}$  is  $\sim 1000 \text{ Pa}$ . It is likely that defects in the crystal match the surface curvature radius during growth.

With regard to the very low water/oil surface tension, it is important to note that only the presence of patches of crystalline cationic nanodiscs at the oil water interface should not

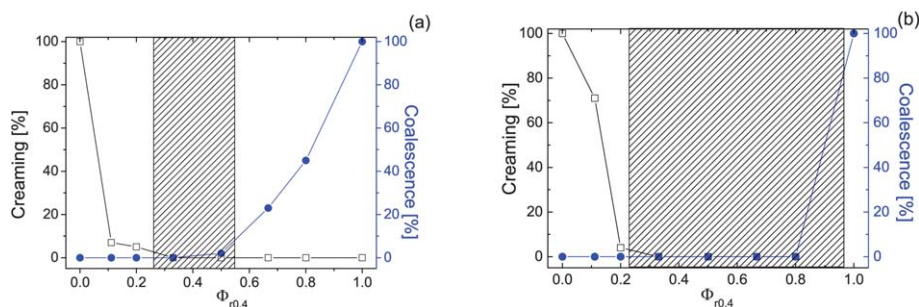


**Fig. 6** Stability against creaming (left hand ordinate) and coalescence (right hand ordinate) for emulsions stabilized by positively charged cationics prepared without (a) and with  $10^{-2}$  M NaCl (b) as a function of the oil/cationic solution ratio. The marked domains correspond to the oil content admissible in formulation for stable emulsions showing neither creaming on the top nor rejection of water at the bottom after more than 90 days of shelf storage.

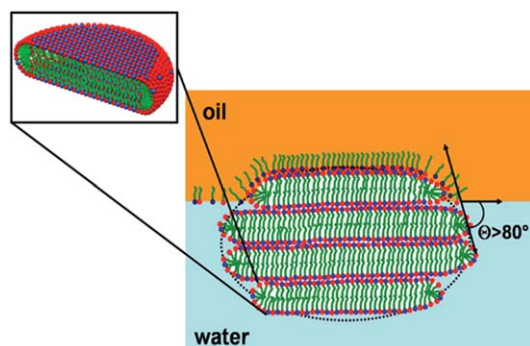


**Fig. 7** Mechanism of stabilization by a stack of cationic nanodiscs. The contact angle of a micro sized oil droplet with the water–oil triple line can be accommodated without deformation. Electric stabilization occurs *via* the outer bilayer, while the effective bending radius of the droplet interface is a combination of nanodiscs rigidity and surface to volume ratio.

produce such low surface tensions at equilibrium, *i.e.* after a few minutes as reported in Fig. 2. The origin of the observed trend of water–oil surface tension could be a consequence of the following points:

1. As shown in Fig. 7, the water/oil interface is covered by a monolayer between the stacks of nanodiscs. According to the segregation model explaining the shapes of such crystals,<sup>36</sup> this monolayer should be enriched by the excess surfactant (negatively charged carboxylic acid on one side ( $r > 0.5$ ), and cationic alkyl trimethylammonium surfactant on the other side ( $r < 0.5$ )). The surface pressure is higher on the positively charged side due to a higher surface charge.

2. Moreover, even in the case of faces of discs near equimolarity, the surface pressure is high and the surface tension is low. One surface phase and two surface phase situations can be distinguished using fluorescence micrographs since they correspond to plateau leveling off in surface pressure isotherms.<sup>37,38</sup> Due to the fact that the linear solvent tetradecane matches the chain length of the last monolayer, the oil can “penetrate” into the monolayer. This situation has been encountered and thoroughly described for lipids at the oil/water interface by ellipsometry and reflectivity in case of lipids where a bulky phosphatidylcholine head-group is involved.<sup>39</sup> According to Thoma and coworkers, even in the liquid condensed phase, linear

matched oil penetration significantly increases the surface pressure. These mechanisms could probably be also the origin of the low surface tension observed for emulsions leading to their long term stability. Moreover, these mechanisms of stabilization are not sensitive to the presence of salt, since molecules are closely packed and the Debye screening length remains larger than the distance between adjacent amphiphiles in the plane of discs, even in the presence of  $10^{-2}$  M of salt.

The zeta-potentials measured indicate that particles have a monolayer on the oil side. This assumption is strengthened by the value frequently measured as triple layers as seen by SANS for the stack.<sup>16</sup> From this one can conclude that the stack of nanodiscs must be covered by a monolayer on the oil side of the stacks, as shown in Fig. 7. If we consider the stack of nanodiscs covering tetradecane droplets as well-defined colloids, those cationic crystals might be designated as self-organized Janus-type particles. The win in surface energy is superior to the entropy of mixing as soon as typical dimensions of charged bilayers are larger than 100 nm.<sup>40</sup> To our knowledge, this is the first time that such a kind of “Janus”-particles produced by segregation of oppositely charged surfactants is used for creating ultra-stable emulsions.

Another interesting feature of the cationic disc used as emulsifier is that the resulting emulsions are insensitive towards the impact of salt. Resilience against the presence of salt is a major problem in emulsion stability. For example, the impact of salt on the stability of emulsion stabilized by globular proteins has been extensively studied because of the large number of important applications.<sup>41</sup> According to the authors, two regimes appear in this type of micro-emulsions: On the one hand, a surfactant-rich regime is observed where only a part of the surfactant is required for covering all droplets and micelles remain in solution. On the other hand, one can also determine a surfactant-poor regime, where the equilibrium size is not dependent on the initial dispersion energy. All emulsions described in this paper are in what one could call the intermediary regime: the vast majority of surfactant is essentially located in the flat particles, but the equilibrium size depends more on initial break-up during preparation in emulsifying mill than on the initial concentration.

For micron-sized droplets with a surface potential in the order of 20 mV as found in the present case, the electrostatic interaction is screened by typically 10 to 100 mM of salt. Above an ion

concentration of 100 mM, ion specific effects come into play leading to an enhanced adsorption of chaotropic ions.<sup>42</sup> Furthermore, ions which adsorb are hydrated and secondary hydration forces come into play at this high salt concentration. The presence of such secondary hydration forces indeed stabilizes emulsion again.<sup>43</sup> In the case described here, the resilience of the Pickering emulsion against screening of electrostatic forces is unique to our knowledge, since the angle of contact as well as the anisometry of the stacks are controlled by non-stoichiometry of the components.

## 5. Conclusion and outlook

Within this work, a simple and robust method describing the preparation of Pickering emulsions is shown and the corresponding mechanism governing the stability of such emulsions has been elucidated in detail. Although the method of stabilizing emulsions by segregation of oppositely charged surfactants has been known for more than 20 years in the field of pharmacy, few papers concerning this topic have been published. This is surprising since the technology was—better said is—still freely accessible, despite of existing patents in the field of emulsions stabilized by oppositely charged surfactants. Furthermore, the resulting catanionic emulsions are extremely difficult to break and their properties can be directly linked to spontaneous “unbreakable” emulsions obtained by diluting a reverse micelle with water. The extensive investigation of the stabilizing mechanism showed that the used nanodiscs have the unique property to break in presence of a hydrophobic interface so that they adsorb at the offered interface *via* a monolayer. Due to this property one can consider such catanionic nanodiscs as self-induced “Janus” particles. In addition, the investigated catanionic emulsions are extremely stable, since the contact angle at the oil–water surface can be adjusted by a suitable choice of the composition of the catanionics (*r*-ratio). Due to the hydrophilic edges of such nanodiscs, it is possible to get contact angles close to 90° which would be the ideal case. For these reasons, catanionic nanodiscs (micro crystals) are a versatile tool to prepare ultra-stable emulsions. This might be interesting for biotechnological applications such as peptides or steroids adsorbed on discs and hydrophobic anti-inflammatory drugs with slow release, as well as for industrial applications as the emulsification of hydrophobic perfumes without alcohol.

## Acknowledgements

A.S. thanks Dr Aliyar Javadi for interfacial tension experiments. N.S. thanks the European Master “Complex Condensed Materials and Soft Matter” (EMASCO-COSOM) and the DFG (French-German Network “Thin films between two and three dimensions”).

## References

- 1 S. U. Pickering, *J. Chem. Soc.*, 1907, **91**, 2001.
- 2 S. Melle, M. Lask and G. Fuller, *Langmuir*, 2005, **21**, 2158.
- 3 S. Abend, N. Bonneke, U. Gutschner and G. Lagaly, *Colloid Polym. Sci.*, 1998, **276**, 730.
- 4 A. Meister, M. Dubois, L. Belloni and T. Zemb, *Langmuir*, 2003, **19**, 7259.
- 5 D. Carrière, L. Belloni, B. Demé, M. Dubois, C. Vautrin, A. Meister and T. Zemb, *Soft Matter*, 2009, **5**, 4983–4990.
- 6 T. Zemb, M. Dubois, B. Demé and T. Gulik-Krzywicki, *Science*, 1999, **283**, 816–819.
- 7 T. Zemb and M. Dubois, *Aust. J. Chem.*, 2003, **56**, 971–979.
- 8 E. Maurer, L. Belloni, T. Zemb and D. Carriere, *Langmuir*, 2007, **23**, 6554–6560.
- 9 A. Khan; E. Marques. *Specialists Surfactant; Blackie Academic and Professional*, an imprint of Chapman & Hall, London, 1997.
- 10 M. Schwuger, *Kolloid. Z. Z. Polym.*, 1971, **243**, 129–135.
- 11 G. May-Alert. Ph.D. thesis, Fachbereich Pharmazie an der Universität Marburg, Germany, 1985.
- 12 G. May-Alert and P. List, *Pharm. Unserer Zeit*, 1986, **15**, 1–7.
- 13 B. Joensson, P. Jokela, A. Khan, B. Lindman and A. Sadaghiani, *Langmuir*, 1991, **7**, 889–895.
- 14 E. Melzer Ph.D. thesis, Universität Braunschweig, 2000.
- 15 A. Lind, J. Andersson, S. Karlsson, P. Agren, P. Bussian, H. Amenitsch and M. Linden, *Langmuir*, 2002, **18**, 1380–1385.
- 16 N. Schelero, H. Lichtenfeld, H. Zastrow, H. Möhwald, M. Dubois and T. Zemb, *Colloids Surf., A*, 2009, **337**, 146–153.
- 17 J.-W. Kim, D. Lee, H. C. Shum and D. A. Weitz, *Adv. Mater.*, 2008, **20**, 3239–3249.
- 18 L. Taisne, P. Walstra and B. Cabane, *J. Colloid Interface Sci.*, 1996, **184**, 378–390.
- 19 M. Dubois and T. Zemb, *Curr. Opin. Colloid Interface Sci.*, 2000, **5**, 27–37.
- 20 M. Dubois, B. Demé, T. Gulik-Krzywicki and T. Zemb, *Nature*, 2001, **411**, 672–675.
- 21 C. Vautrin, T. Zemb, M. Schneider and M. Tanaka, *J. Phys. Chem. B*, 2004, **108**, 7986–7991.
- 22 M. Dubois, B. Demé, T. Gulik-Krzywicki and T. Zemb, *C.R. Acad. Sci. Paris*, 1998, **Série IK**, 567–575.
- 23 A. Javadi, J. Kraegel, P. Pandolfini, G. Loglio, V. Kovalchuk, E. Aksenenko, F. Ravera, L. Liggieri and R. Miller, *Colloids Surf., A*, 2010, **365**, 62.
- 24 Y. Michina, D. Carriere, C. Mariet, M. Moskura, P. Berthault, L. Belloni and T. Zemb, *Langmuir*, 2009, **25**, 698–706.
- 25 A. Stocco, D. Carriere, M. Cottat and D. Langevin, *Langmuir*, 2010, **26**, 10663–10669.
- 26 K. Ciunel, M. Armelin, G. H. Findenegg and R. von Klitzing, *Langmuir*, 2005, **21**, 4790–4793.
- 27 J. K. Beattie, A. M. Djerdjev and G. G. Warr, *Faraday Discuss.*, 2009, **141**, 31–39.
- 28 B. Binks and J. H. Clint, *Langmuir*, 2002, **18**, 1270–1273.
- 29 F. Talens-Alession, *J. Phys. Chem. B*, 2009, **113**, 9779–9785.
- 30 K. A. Connors and K. A. Wright, *Anal. Chem.*, 1989, **61**, 194.
- 31 P. Lavi and J. Marmur, *J. Colloid Interface Sci.*, 2000, **230**, 107.
- 32 A. Zdziennicka and B. Janczuk, *J. Colloid Interface Sci.*, 2010, **349**, 374.
- 33 P. Pieranski, *Phys. Rev. Lett.*, 1980, **45**, 569–572.
- 34 J. Weiss, *Curr. Prot. Food Analytical Chem.*, 2002, D3.4.1–D3.4.17.
- 35 N. Delorme, M. Dubois, S. Garnier, A. Laschewsky, R. Weinkamer, T. Zemb and A. Fery, *J. Phys. Chem. B*, 2006, **110**, 1752–1758.
- 36 M. Dubois, V. Lizunov, A. Meister, T. Gulik-Krzywicki, J.-M. Verbavatz, E. Perez, J. Zimmerberg and T. Zemb, *Proc. Natl. Acad. Sci. U. S. A.*, 2004, **101**, 15082–15087.
- 37 M. Thoma and H. Möhwald, *J. Colloid Interface Sci.*, 1994, **92**, 340–349.
- 38 M. Thoma, T. Pfohl and H. Möhwald, *Langmuir*, 1995, **11**, 2881–2888.
- 39 M. Thoma, M. Schwendler, H. Baltes, C. A. Helm, T. Pfohl and H. R. Möhwald, *Langmuir*, 1996, **12**, 1722–1728.
- 40 M. Dubois, L. Belloni, T. Zemb, B. Demé and T. Gulik-Krzywicki, *Prog. Colloid Polym. Sci.*, 2000, **115**, 238–242.
- 41 S. Tcholakova, N. Denkov, I. Ivanov and B. Campbell, *Adv. Colloid Interface Sci.*, 2006, **123–126**, 259–293.
- 42 *Specific Ion Effects*, ed. W. Kunz, World Scientific Publishing, 2010.
- 43 V. Parsegian and T. Zemb, *Curr. Op. Colloids Interfaces*, 2011, DOI: 10.1016/j.cocis.2011.06.010.